Journal of Infection 92 (2026) 106754

Contents lists available at ScienceDirect

Journal of Infection

journal homepage: www.elsevier.com/locate/jinf

Viruses and Viral Diseases

Early antiretroviral therapy shapes the immunometabolic landscape without reducing the intact HIV reservoir

Paula Suanzes [a,b,c,1], Judith Grau-Expósito [b,1], Jordi Navarro [a,b], Silvia Chafino [d,e], Anna Rull [d,e], Ariadna Rando-Segura [f], Patricia Álvarez-López [a,b], Vicente Descalzo [a,b], Jorge N. García [a,b], Arnau Monforte [a,b], Adrian Curran [a,b], Joaquín Burgos [a,b], Bibiana Planas [b], Marta Sanchiz [b], Meritxell Genescà [b], Vicenç Falcó [a,b,c], María José Buzón [b,*]

[a] Infectious Diseases Department, Vall d'Hebron Hospital Universitari, Vall d'Hebron Barcelona Hospital Campus, Barcelona, Spain
[b] Infectious Diseases Department, Vall d'Hebron Institut de Recerca (VHIR), Instituto de Investigación Sanitaria Hospital Universitari Vall d'Hebron (IIS IR-HUVH), Universitat Autònoma de Barcelona, Barcelona, Spain
[c] Departament de Medicina, Universitat Autònoma de Barcelona, Bellaterra, Spain
[d] Institut de Recerca Biomèdica Catalunya Sud, Hospital Universitari de Tarragona Joan XXIII (HJ23), Tarragona, Spain
[e] Centro de Investigación Biomédica en Red de Enfermedades Infecciosas (CIBERINFEC), Instituto de Salud Carlos III, Madrid, Spain
[f] Microbiology Department, Vall d'Hebron Hospital Universitari, Vall d'Hebron Barcelona Hospital Campus, Barcelona, Spain

ARTICLE INFO

Article history:
Accepted 23 April 2026
Available online 28 April 2026

Keywords:
HIV
HIV infections
HIV reservoir
Inflammation
Immunometabolism
Metabolomics
Cytokines
HIV seroconversion

SUMMARY

Objectives: We assessed the effect of early ART during acute HIV infection on reservoir dynamics, cytokine profile, and T-cell metabolism.
Methods: We studied a longitudinal cohort of PWH starting ART during early (ET) or chronic (CT) infection, and a cross-sectional cohort including matched ET and CT participants (≥36 months virologically suppressed) and HIV-negative controls. We analysed total HIV DNA, intact and defective proviruses, cell-associated HIV RNA, plasma cytokines, and metabolomic profiles of $CD4^+$ and $CD8^+$ T-cells.
Results: Over 75% of ET participants started ART in Fiebig stages IV–VI. Early ART was associated with lower total HIV DNA and cell-associated RNA. Although intact proviruses were similar between groups, they represented a larger proportion of the reservoir in ET participants. Worse pre-ART immune status correlated with a larger and more transcriptionally active reservoir. Regulatory, inflammatory, and homeostatic cytokines negatively correlated with the intact reservoir, particularly in CT participants. Metabolomic profiling of T-cells demonstrated ART timing-dependent alterations in several metabolic pathways. Metabolites involved in glycolysis, amino-acid metabolism, and polyol pathways positively correlated with HIV transcription in $CD4^+$ T-cells, especially in CT participants.
Conclusion: Early ART limits the HIV reservoir size, shapes its composition, and influences immunometabolic pathways, though it might not be enough to reduce the intact reservoir.

Introduction

Current antiretroviral therapy (ART) has dramatically improved health outcomes and quality of life of people with HIV (PWH) by achieving viral suppression, enabling immune recovery, and preventing HIV transmission.[1–5] However, the persistence of a viral reservoir remains the main barrier to HIV cure.[6]

The HIV reservoir is established in the early stages of acute HIV infection (AHI),[7,8] but the start of ART heavily influences its composition, as a large proportion of the viral sequences that persist despite ART-induced viral suppression are derived from cells infected shortly before treatment initiation.[9] Although starting ART during AHI does not completely prevent the seeding of the viral reservoir,[7] it has been associated with a faster decay rate[10] and a smaller overall reservoir size.[11,12] Immunological status may also play a role, as individuals with higher $CD4^+$ T-cell counts who start ART during AHI show a faster decay of the HIV reservoir.[13] In chronic

* Correspondence to: Infectious Diseases Research Group, Vall d'Hebron Institut de Recerca (VHIR), Vall d'Hebron Hospital Universitari, Vall d'Hebron Barcelona Hospital Campus, Passeig Vall d'Hebron 119-129, 08035 Barcelona, Spain.
E-mail address: mariajose.buzon@vhir.org (M.J. Buzón).
[1] PS and JGE contributed equally to this work.

https://doi.org/10.1016/j.jinf.2026.106754

HIV infection, intact (replication-competent) proviruses appear to decline faster than defective ones during ART.[14–16] While several studies have explored changes in viral reservoir composition following ART initiation during AHI,[12,13] we still do not fully understand how early ART impacts the composition and dynamics of the viral reservoir.

Despite the benefits of ART, virologically suppressed PWH continue to exhibit sustained, albeit reduced, immune activation and inflammation.[17,18] This chronic pro-inflammatory state has been linked to several non-AIDS comorbidities such as cardiovascular disease, neurocognitive impairment, and non-AIDS defining malignancies.[19,20] Although ART reduces several plasma inflammatory markers[17,21–23] and some data suggest that early ART during AHI may further impact chronic inflammation,[21,24,25] we still lack longer term, well-matched comparisons with people treated during chronic HIV infection.

Metabolic reprogramming of immune cells during HIV infection contributes to persistent immune activation, chronic inflammation, and immune dysfunction.[26] Activated immune cells display a metabolomic profile characterized by the activation of high-energy pathways such as glycolysis.[27] Cells with higher metabolic activity are also more susceptible to HIV infection.[28] Over time, this chronic activation results in metabolic exhaustion and impaired immune effector function.[26,29] A recent study suggests that early ART during AHI preserves nutrient uptake and mitochondrial mass in $CD4^+$ T-cells,[30] but it remains to be explored whether early ART also influences other metabolic pathways.

In this study, we aimed to assess the impact of initiating ART during early or chronic HIV infection on the composition and decay of the viral reservoir, as well as on plasma inflammatory markers and on the metabolomic profile of $CD4^+$ and $CD8^+$ T-cells.

Methods

Study design and participants

The Vall d'Hebron Acute HIV Infection (VHAHI) cohort is an ambispective cohort that includes participants aged 18 years or older with confirmed acute HIV-1 infection followed at the HIV outpatient clinic of Hospital Universitari Vall d'Hebron, Barcelona (Spain),[31] with 203 participants enrolled to date. All participants in the VHAHI cohort are invited to provide blood samples prior to ART initiation and at regular intervals during follow-up. Additionally, during 2017–2019 newly diagnosed PWH, regardless of acute or chronic infection, were also invited to provide regular blood samples.

In this study, we performed longitudinal and cross-sectional analyses. Participants were classified into three groups: early treated (ET), treated during chronic HIV infection (CT), and HIV-negative controls (HNC). The ET group consisted of participants enrolled in the VHAHI cohort who started ART within 180 days of the estimated date of infection (EDI). The CT group included individuals who initiated ART during the chronic phase of HIV infection. The HNC group consisted of individuals with a negative HIV test and without chronic medical conditions. Specific criteria used to classify HIV infection as acute or chronic are described in the *Definitions* section.

For the longitudinal analysis, we included ET and CT participants with at least 36 months of follow-up and available blood samples at five time points: T_0 (before starting ART), T_1 (median: 1 month after ART initiation), T_2 (median: 8 months after ART), T_3 (median: 44 months after ART), T_4 (median: 71 months after ART). Individuals who interrupted ART during follow-up or who did not have a minimum of two available samples (one at T_0, and at least one during follow-up) were excluded. We quantified total HIV DNA and frequencies of intact and defective proviruses in $CD4^+$ T-cells from peripheral blood mononuclear cells (PBMCs) at all available time points.

For the cross-sectional analyses, we recruited 23 ET and 20 CT participants (cross-sectional cohort A), all of whom had been on ART and virologically suppressed for at least 36 months. We then selected the ET participants from cohort A and identified sex- and age-matched (±5 years) CT individuals and HNC. ET and CT participants were additionally matched by pre-ART $CD4^+$ T-cell count, time on ART at inclusion, and duration of virological suppression at inclusion. When no CT candidate with a similar pre-ART $CD4^+$ T-cell count was available, we selected the closest eligible match who met all the other criteria. ET individuals for whom no matched CT controls could be found were excluded. This resulted in a matched cross-sectional cohort (cohort B) comprising 13 ET participants matched to 13 CT individuals (all virologically suppressed for at least 36 months) and 13 HNC. In both cross-sectional cohorts, we obtained blood samples and quantified total HIV DNA, frequencies of intact and defective proviruses and cell-associated (CA) HIV RNA in $CD4^+$ T-cells isolated from PBMCs. In matched cohort B we additionally measured plasma cytokine levels. In a subset of 11 matched ET-CT-HNC trios with available samples, we also characterized the metabolomic profiles of $CD4^+$ and $CD8^+$ T-cells.

The study was approved by the hospital ethics committee (PR(AG) 270/2015, PR(AG)377/2019, PR(AG)358/2021, and PR(AG)315/2023) and followed the ethical principles based on the latest version of the Declaration of Helsinki. Written informed consent was obtained from all participants. The processing of the participants' personal data collected in the studies complies with the Data Protection Act 1998 and with the European Directive on the Privacy of Data.

Definitions

AHI infection was defined as (a) negative third- or fourth-generation assay for HIV-1 and positive HIV-1 plasma viral load (VL); (b) positive or negative third- or fourth-generation assay for HIV-1, negative or undetermined (< 2 envelope bands) Western blot or LIA, positive serum p24 antigen, and positive plasma HIV-1 VL; (c) positive third- or fourth-generation assay for HIV-1, and negative, undetermined or positive without p31 band Western blot or LIA, and positive HIV-1 plasma VL; or (d) HIV-1 seroconversion in the last 6 months (evidence of a negative HIV-1 test in the last 180 days). We calculated the estimated date of infection (EDI) using Fiebig staging[32] and previous HIV negative tests, as a simplified approach based on diagnostic staging and testing intervals: 15 days before the first positive HIV test in Fiebig stage I, 20 days before the first positive HIV test in Fiebig stage II, 24 days before the first positive HIV test in Fiebig stage III, 29 days before the first positive HIV test in Fiebig stage IV, and 99 days before the first positive HIV test in Fiebig stage V. In Fiebig stage VI we defined the EDI as the midpoint between 99 days before the first positive HIV test and the date of the last HIV negative test. When Fiebig stage was unknown, we defined the EDI as the midpoint between the first positive HIV test and the last negative HIV test. Chronic HIV infection was defined as a positive fourth-generation assay for HIV-1 and a positive Western blot or LIA with positive p31 band in the absence of a HIV negative test or symptoms of acute retroviral syndrome within the year before seroconversion. EDI was not calculated in participants with chronic HIV infection.

Viral suppression was defined as HIV VL < 50 copies/mL. Blips, defined as isolated determinations of HIV VL between 50 and 400 copies/mL, were not considered loss of viral suppression. Two consecutive determinations of detectable HIV VL below 200 copies/mL followed by a third determination < 50 copies/mL were also not considered loss of viral suppression.

Study variables and data collection

Demographic, epidemiological, HIV-related variables (date of diagnosis, date of last negative HIV test, Fiebig stage, date of ART initiation, ART regimens), and $CD4^+$ and $CD8^+$ T-cell counts and HIV-

1 VL at diagnosis, prior to ART initiation, and during follow-up were collected. ART treatment selection was left to the treating physician's discretion.

Virological analyses

HIV-1 serology and viral load measurements were performed using validated commercial assays available at the time of testing. During the study period, several HIV-1 antigen/antibody immunoassays and real-time PCR platforms were used, reflecting routine methodological updates in the laboratory. All assays were conducted according to manufacturers' instructions and standard quality assurance procedures.

Isolation of PBMCs

PBMCs were isolated from blood by Ficoll-Paque density gradient centrifugation and cryopreserved in liquid nitrogen. $CD8^+$ T-cells were purified from PBMCs using a positive selection kit (CD8 MicroBeads, Miltenyi Biotec, Bergisch Gladbach, Germany). $CD4^+$ T-cells were isolated using a negative selection kit (MagniSort Human $CD4^+$ T Cell Enrichment; eBioscience/Invitrogen, Thermo Fisher Scientific, MA, USA). Purified cells were lysed in a Proteinase K-containing lysis buffer at 55 °C overnight, followed by heat inactivation at 95 °C for 5 min.

Intact proviral DNA assay (IPDA)

IPDA was conducted as described before[33] on lysed $CD4^+$ T-cells isolated from PBMCs using specific primers and probes targeting the Ψ (psi) HIV gene (HIV-1 Ψ forward 50 5'-CAGGACTCGGCTTGCTG AAG-3', HIV-1 Ψ reverse 5'-GCACCCATCTCTCTCCTTCTAGC-3' and probe 5' 6-FAM-TTTTGGCGTACTCACCAGT-MGBNFQ-3') and the env HIV gene (HIV-1 env forward 5'-AGTGGTGCAGAGAGAAAAAAGAGC-3', HIV-1 env reverse 5'-GTCTGGCCTGTACCGTCAGC-3', HIV-1 env intact probe 5'-VIC-CCTTGGGTTCTTGGGA-MGBNFQ-3', and HIV-1 anti-Hypermutant env probe 5'-CCTTAGGTTCTTAGGAGC-MGBNFQ-3'). For participants in whom amplification of the HIV-1 env gene failed, a second set of primers and probe was used, as described by Kinloch et al.[34] These were as follows: secondary HIV-1 env forward primer 5'-ACTATGGGCGCAGCGTC-3', secondary HIV-1 env reverse primer 5'-CCCCAGACTGTGAGTTGCA-3' and secondary HIV-1 env probe 5'-VIC-CTGGCCTGTACCGTCAG- MGBNFQ-3'. The human RPP30 gene served as a reference for cell input normalization. Samples were analysed using a QIAcuity One 2 plex System (Qiagen, Hilden, Germany). Intact provirus measurements were corrected for DNA shearing, and samples with excessive shearing were excluded from the final analysis. Proviruses with hypermutations and/or 3' deletions or with 5' deletions were considered defective.

Quantification of proviral HIV DNA by quantitative PCR (qPCR)

The total HIV DNA in the cell lysates was quantified by qPCR using primers and a probe specific for the 1-LTR region of HIV (LTR forward: 5′-TTAAGCCTCAATAAAGCTTGCC-3′, LTR reverse: 5′-GTTCG GGCGCCACTGCTAG-3′, and probe: 5′/56-FAM/CCAGAGTCA/ZEN/CAC AACAGACGGGCA/31ABkFQ/3′). Reactions were carried out using TaqMan™ Gene Expression Master Mix (Thermo Fisher Scientific, MA, USA). The CCR5 gene was used as a reference for cell input normalization. DNA quantification was performed using a standard curve, and values were normalized to one million $CD4^+$ T-cells. Samples were analyzed using an Applied Biosystems QuantStudio 5 system (Thermo Fisher Scientific, MA, USA).

Quantification of HIV cell-associated (CA) RNA

A minimum of 1 million cells were subjected to RNA extraction using the NZY Total RNA Isolation Kit (NZYtech, Lisbon, Portugal). RNA was reverse transcribed with SuperScript III (Invitrogen, Thermo Fisher Scientific, MA, USA) in accordance with the instructions provided by the manufacturer, and complementary DNA was quantified by qPCR with primers and probes specific for the HIV long terminal repeat-gag region. Copies of HIV RNA were quantified with an HIV RNA standard, and values were normalized to micrograms of RNA of the original sample.

Cytokines

We measured cytokine levels in plasma (pg/mL) using the Olink® Target 48 Cytokine panel (Olink, Uppsala, Sweden). The panel measures 45 human proteins associated with inflammation: C-X-C motif chemokine 11 (CXCL11 or I-TAC), tumor necrosis factor ligand superfamily member 12 (TNFSF12 or TWEAK), interleukin-33 (IL-33), pro-epidermal growth factor (EGF), protransforming growth factor alpha (TGF-α), lymphotoxin-alpha (LTA or TNF-β), tumor necrosis factor (TNF-α), interferon gamma (IFN-γ), interleukin-1 beta (IL-1β), C-X-C motif chemokine 10 (CXCL10 or IP-10), interstitial collagenase (MMP-1), granulocyte-macrophage colony-stimulating factor (GM-CSF), interleukin-4 (IL-4), interleukin-6 (IL-6), macrophage colony-stimulating factor 1 (M-CSF), granulocyte colony-stimulating factor (G-CSF), interleukin-8 (IL-8), C-C motif chemokine 3 (CCL3 or MIP-1α), interleukin-7 (IL-7), C-C motif chemokine 4 (CCL4 or MIP-1β), C-C motif chemokine 2 (CCL2 or MCP-1), oncostatin-M (OSM), hepatocyte growth factor (HGF), vascular endothelial growth factor A (VEGF-A), interleukin-10 (IL-10), interleukin-13 (IL-13), macrophage metalloelastase (MMP-12), interleukin-15 (IL-15), stromal cell-derived factor 1 (CXCL12 or SDF-1α), FMS-related tyrosine kinase 3 ligand (FLT3L), tumor necrosis factor ligand superfamily member 10 (TNFSF10 or TRAIL), eotaxin (CCL11), interleukin-2 (IL-2), oxidized low-density lipoprotein receptor 1 (OLR1 or LOX-1), C-C motif chemokine 8 (CCL8 or MCP-2), C-C motif chemokine 4 (CCL7 or MCP-3), C-X-C motif chemokine 9 (CXCL9 or MIG), interleukin-18 (IL-18), interleukin-17A (IL-17A), interleukin-27 (IL-27), thymic stromal lymphopoietin (TSLP), interleukin-17F (IL-17F), C-C motif chemokine 13 (CCL13 or MCP-4), C-C motif chemokine 19 (CCL19 or MIP-3β), and interleukin-17C (IL-17C).

Metabolomic analysis

For metabolomics, a protein precipitation extraction was performed by 0.5 mL of methanol:water (8:2) containing internal standard mixture (succinic acid-d4, myristic acid-d27, glycerol13C3 and D-glucose13C6) to cell pellets (½ million cells) and homogenized with an ultrasonic probe (3 cycles, 20% amplitude, 10 s/cycle) for 1 min and incubated at −20 °C for 30 min. Then, the samples were centrifuged at 15,000 rpm, and the supernatant was evaporated to dryness before compound derivatization (methoximation and silylation). The derivatized compounds were analysed using a 7200 gas chromatography-quadrupole time-of-flight mass spectrometer (GC-QTOF) from Agilent Technologies (Santa Clara, CA, USA). The chromatographic separation was based on the Fiehn Method, using a J& W Scientific HP5-MS (30 m × 0.25 mm i.d., 0.25 µm film capillary column and helium as carrier gas, using an oven program from 60 to 325 °C. Ionization was done by electronic impact (EI), with an electron energy of 70 eV and operated in full scan mode. In addition to targeted compounds from central carbon metabolism, which were quantified using internal standard calibration curves, a screening for the identification of more metabolites was performed by matching

their EI mass spectrum and retention time to the metabolomic Fiehn library (from Agilent), which contains more than 1.400 metabolites. After putative identification of metabolites, these were semi-quantified in terms of internal standard response ratio. A total of 47 metabolites were identified in both $CD4^+$ and $CD8^+$ T-cells.

Statistical analysis

Categorical variables were expressed as absolute frequencies and percentages, and continuous variables as medians and interquartile ranges (IQR). Fisher's exact test, the Mann-Whitney *U* test, and the Kruskal-Wallis test followed by post-hoc Dunn's multiple comparisons test were used for group comparisons. To account for multiple testing, false discovery rate (FDR) control was applied using the two-stage linear step-up procedure of Benjamini, Krieger, and Yekutieli (Q = 1%). We evaluated if the decay of total, intact and defective HIV DNA was better described by a single-phase linear model or a segmented (two-phase) linear regression model using the extra sum-of-squares F test. We used Spearman's rank correlation to assess relationships between reservoir measures, clinical parameters, cytokine levels, and metabolites. Statistical analyses were performed using IBM SPSS statistics software for Windows (Version 21; IBM, Armonk, NY, USA) and GraphPad Prism (Version 10.6.1; Boston, MA, USA). For the metabolomic analysis, the ROUT test (Q = 1%) was used for identifying outliers in raw data, which were subsequently excluded from the analysis. Supervised multivariate analysis, including partial least squares discriminant analysis (PLS-DA) and Random Forest, were performed using MetaboAnalyst 6.0 software (web-based platform, accessible at https://www.metaboanalyst.ca) to classify samples. All tests were two-tailed and a *p*-value of < 0.05 was considered significant. We used GraphPad Prism and MetaboAnalyst 6.0 software for graphic representations.

Results

Longitudinal viral reservoir dynamics and changes in composition

We performed a longitudinal analysis including 14 ET participants and 10 CT participants. Median time from EDI to ART initiation was 46 days (34.3–111.5) in the ET group, with 78.6% of participants classified in Fiebig stages IV–VI. Pre-ART HIV viral load was higher in the ET group, but there were no significant differences in pre-ART $CD4^+$ and $CD8^+$ T-cell counts, or in the pre-ART $CD4^+/CD8^+$ ratio (Table 1).

To assess the differences in the decay and composition of the HIV reservoir between ET and CT participants, we measured total HIV DNA and frequencies of intact and defective proviruses. As shown in Fig. 1, after the start of ART all viral forms declined over time in both cohorts. We explored whether the decay of total, intact and defective HIV DNA fitted a single-phase linear model or a segmented two-phase linear regression model. In both ET and CT groups, total HIV DNA declined in a biphasic pattern (ET: $F(1, 48) = 8.73$, $p = 0.005$; CT: $F(1, 28) = 5.02$, $p = 0.033$) characterized by a rapid and steep initial decline followed by a much slower decay in the second phase (Fig. 1A). There were no differences in the steeper initial decay between ET and CT participants (Fig. 1B). However, in the second phase we observed a continuous decay in ET participants ($t_{1/2}$ = 131.9 months) compared to a plateau in CT participants ($t_{1/2}$ = infinite) (Fig. 1A), although the difference between slopes did not reach statistical significance (Fig. 1B). Regarding intact HIV DNA, decay was also biphasic in ET individuals ($F(1, 51) = 6.34$, $p = 0.015$) but followed a linear pattern in CT participants (Fig. 1C). After the initial faster decline in ET participants, intact viral forms continued to slowly decline in both groups, with similar half-lives (72.3 and 74.1 months, respectively) and no significant differences (Fig. 1C and D). Defective proviruses showed a biphasic decline in ET and CT participants (Fig. 1E and G). This pattern was observed for both hypermutated and/or 3' deleted forms (ET: $F(1, 51) = 17.46$, $p < 0.001$; CT: $F(1, 23) = 9.00$, $p = 0.006$) and for 5' deleted forms (ET: $F(1, 51) = 20.74$, $p < 0.001$; CT: $F(1, 24) = 10.21$, $p = 0.004$). Although first-phase decay rates were similar between ET and CT groups (Fig. 1F and H), in the second phase the decline of defective proviruses plateaued in CT participants ($t_{1/2}$ = 1105 months for hypermutated and/or 3' deleted forms and $t_{1/2}$ = 519.4 months for 5' deleted forms), whereas continuous decay was observed in ET individuals ($t_{1/2}$ = 107.1 months for hypermutated and/or 3' deleted forms and $t_{1/2}$ = 87.3 months for 5' deleted forms) (Fig. 1E–H). Overall, intact HIV-DNA decay was very similar between ET and CT participants. However, for both total and non-intact reservoir measurements, the second phase of viral decay stalled in CT participants.

Viral reservoir size and composition after prolonged ART

We then aimed to assess whether the timing of ART initiation influenced the size and composition of the HIV reservoir after an extended period on ART. To this end, we performed a cross-sectional analysis including 23 ET participants and 20 CT participants who had been at least 36 months on ART and virologically suppressed (cross-sectional cohort A, Table 2). The median time from EDI to the start of ART was 73 days (39–116) in the ET group, 78.3% of ET participants were classified in Fiebig stages IV-VI. As expected, pre-ART HIV VL was higher in the ET group, but there were no significant differences between ET and CT participants in sex, age, pre-ART or at inclusion $CD4^+$ and $CD8^+$ T-cell counts, pre-ART or at inclusion $CD4^+/CD8^+$ ratio, nadir $CD4^+$ T-cell counts, or ART regimens. Participants had been on ART for a median of 73 months (61–97) and had maintained virological suppression for a median of 69 months (55–91), without significant differences between groups.

We quantified total HIV DNA, intact and defective proviruses, and assessed viral transcription by measuring CA RNA. Total HIV DNA and defective hypermutated and/or 3' deleted forms were more frequent in CT than in ET participants (Fig. 2A). Interestingly, intact HIV DNA remained similar between ET and CT groups (Fig. 2A). We next quantified the relative proportions of the different viral DNA forms in each cohort. The fraction of intact proviruses within the total HIV DNA pool was significantly higher in the ET group (18.0% vs. 8.7%) (Fig. 2B). Moreover, CA HIV RNA was increased in CT compared to ET participants (Fig. 2C). Overall, in this cohort of participants treated at different stages, we found that prolonged ART initiated during AHI was associated with lower levels of total HIV DNA and CA RNA. Unexpectedly, while intact HIV DNA levels were similar between groups, intact proviruses constituted a significantly larger proportion of the total HIV DNA pool in ET than in CT participants, highlighting a qualitative difference in the reservoir despite similar per-cell levels.

We then assessed the relationship between pre-ART $CD4^+/CD8^+$ ratio and the size and composition of the viral reservoir. Both total HIV DNA and CA RNA levels were significantly increased in PWH who started ART with a low pre-ART $CD4^+/CD8^+$ ratio (< 0.5) compared to those with a pre-ART $CD4^+/CD8^+$ ratio ≥ 0.5) ($p = 0.004$ and $p = 0.015$ respectively; Table S1). No significant differences were observed in intact or defective HIV viral forms between participants with a pre-ART $CD4^+/CD8^+$ ratio < 0.5 versus ≥ 0.5 (Table S1).

Furthermore, we observed a negative correlation between pre-ART $CD4^+/CD8^+$ ratio and total HIV DNA ($r_s = -0.58$, $p < 0.001$, n = 37), hypermutated and/or 3' deleted ($r_s = -0.39$, $p = 0.017$, n = 38), 5' deleted HIV DNA ($r_s = -0.37$, $p = 0.022$, n = 38), and CA HIV RNA ($r_s = -0.44$, $p = 0.005$, n = 39). Pre-ART $CD4^+$ T-cell counts negatively

Table 1
Demographic and immunovirological characteristics of participants included in the longitudinal cohort.

	Total (n = 24)	Early treated (n = 14)	Chronically treated (n = 10)	*p*-value[a]
Age, years	28 (24.3–38.8)	27.5 (23–36.5)	32.5 (25.5–40.3)	0.44
Sex, male	20 (83.3)	13 (92.9)	7 (70)	0.27
Geographic origin				0.13
Spain	16 (66.7)	11 (78.6)	5 (50)	
Africa	1 (4.2)	0 (0)	1 (10)	
Central/South America	6 (25)	2 (14.3)	4 (40)	
Europe (excluding Spain)	1 (4.2)	1 (7.1)	0 (0)	
HIV-1 subtype				0.16
B	21 (87.5)	13 (92.9)	8 (80)	
F	2 (8.3)	0 (0)	2 (10)	
Recombinant forms	1 (4.2)	1 (7.1)	0 (0)	
Pre-ART HIV-1 VL, copies/mL	317,500 (61,350–2,540,000)	1,033,500 (271,000–8,412,500)	83,150 (29,475–305,250)	0.002
Pre-ART $CD4^+$ T- cell count, cells/μL	475 (370–608)	555 (375–623)	430 (355–605)	0.44
Pre-ART $CD8^+$ T-cell count, cells/μL	975 (705–1288)	925 (598–1220)	975 (875–1428)	0.44
Pre-ART $CD4^+/CD8^+$ ratio	0.51 (0.34–0.69)	0.55 (0.43–0.86)	0.47 (0.28–0.63)	0.29
Fiebig stage	NA		NA	NA
I		0 (0)		
II		1 (7.1)		
III		2 (14.3)		
IV		5 (35.7)		
V		2 (21.4)		
VI		2 (21.4)		

Results are expressed as number (%) or median (IQR). ART, antiretroviral therapy; NA, not applicable; VL, viral load.
Percentages may not sum to 100 due to rounding.
[a] *p*-values are the result of the Mann-Whitney *U* test for continuous variables and Fisher's exact test for categorical variables.

correlated with total HIV DNA (r_s = −0.38, p = 0.018, n = 38), intact HIV DNA (r_s = −0.40, p = 0.011, n = 39), hypermutated and/or 3' deleted HIV DNA (r_s = −0.32, p = 0.045, n = 39), and CA HIV RNA (r_s = −0.39, p = 0.012, n = 40). We found no correlation between pre-ART HIV VL, current $CD4^+$ and $CD8^+$ T-cell counts, or the current $CD4^+/CD8^+$ ratio and reservoir or CA RNA measures (Fig. 2D). These results indicate that a worse pre-ART immune status is associated with a larger and more transcriptionally active HIV reservoir despite viral suppression.

Plasma cytokine levels according to timing of ART initiation

Next, we evaluated whether inflammatory marker profiles differed according to the timing of ART initiation or HIV status by measuring cytokine levels in plasma samples. We included 13 ET participants and matched them across multiple parameters (detailed in the *Methods* section) to 13 CT and 13 HNC (matched cross-sectional cohort B). Both ET and CT participants had been at least 36 months on ART and virologically suppressed. Demographic and immunovirological characteristics of participants in the matched cross-sectional cohort are shown in Table 3. The median time from EDI to the start of ART was 73 days (40.5–166.5) in the ET group. There were no significant differences between ET and CT participants in sex, age, pre-ART or at inclusion $CD4^+$ and $CD8^+$ T-cell counts, pre-ART or at inclusion $CD4^+/CD8^+$ ratio, nadir $CD4^+$ T-cell counts, pre-ART HIV VL, or ART regimens. All participants started a 3-drug combination regimen consisting of 2 nucleoside reverse transcriptase inhibitors (NRTI) plus a third agent, except for one matched ET-CT pair who started a 2-drug combination regimen (dolutegravir plus lamivudine). Participants had been on ART for a median of 77.5 months (63.5–109) and virologically suppressed for a median of 74 months (59.5–105), without significant differences between groups.

For 42 of the 45 cytokines measured, no differences were observed among HNC, ET, and CT groups, nor between HNC and all PWH (Fig. S1). In the unadjusted analysis, IL-10 levels were increased in the ET group compared to CT participants and HNC and were also elevated in PWH versus HNC. MMP-1 and MIG levels were higher in PWH than in HNC, but without differences between ET and CT individuals. However, none of these differences remained significant after FDR correction. Overall, plasma cytokine levels were largely similar between ET and CT participants, with only limited nominal differences in IL-10.

Next, we examined potential associations between cytokine levels and HIV reservoir measures. In general, seven cytokines (MCP-2, IL-2, IL-1β, TWEAK, IL-7, MCP-4, and IL-10) showed a negative correlation with total HIV DNA levels (Fig. 3A). Notably, within the CT group, we observed stronger negative correlations between reservoir size and several cytokines (IL-2, IL-7, IL-10, IL-8, and EGF). Particularly, IL-8, MIP-1β (proinflammatory), IL-10 (regulatory), SDF-1α (homeostatic and chemotactic), and IL-7 (homeostatic and lymphopoietic) were more tightly associated with intact HIV DNA in CT participants (Fig. 3A and B), emphasizing their potential link to the replication-competent reservoir in this group. Of these, only IL-10 was upregulated in ET participants (Fig. 3C). Conversely, among ET participants, only I-TAC, a pro-inflammatory chemokine, was negatively correlated with intact HIV DNA (Fig. 3A). Together, these findings suggest that both inflammatory and homeostatic pathways may contribute to modulating HIV persistence, with more associations observed in participants who initiated ART during the chronic phase.

Metabolomic profiles of $CD4^+$ and $CD8^+$ T-cells according to timing of ART initiation

As ART timing may influence immune cell metabolism, we analysed the metabolomic profiles of $CD4^+$ and $CD8^+$ T-cells from 33 paired participants with samples available in the matched cross-sectional cohort B (11 ET, 11 CT, and 11 HNC). To enhance statistical robustness and minimize bias, results that met predefined outlier detection criteria were excluded from the analysis. PLS-DA revealed modest separation of metabolic profiles between groups in both $CD4^+$ and $CD8^+$ T-cells (Fig. S2). Next, we performed hierarchical clustering of the metabolomic profiles of $CD4^+$ and $CD8^+$ T-cells across the three groups, which is displayed as a heatmap illustrating the relative abundance of each metabolite (Fig. 4A and B). The dendrogram revealed clustering patterns that largely separated ET,

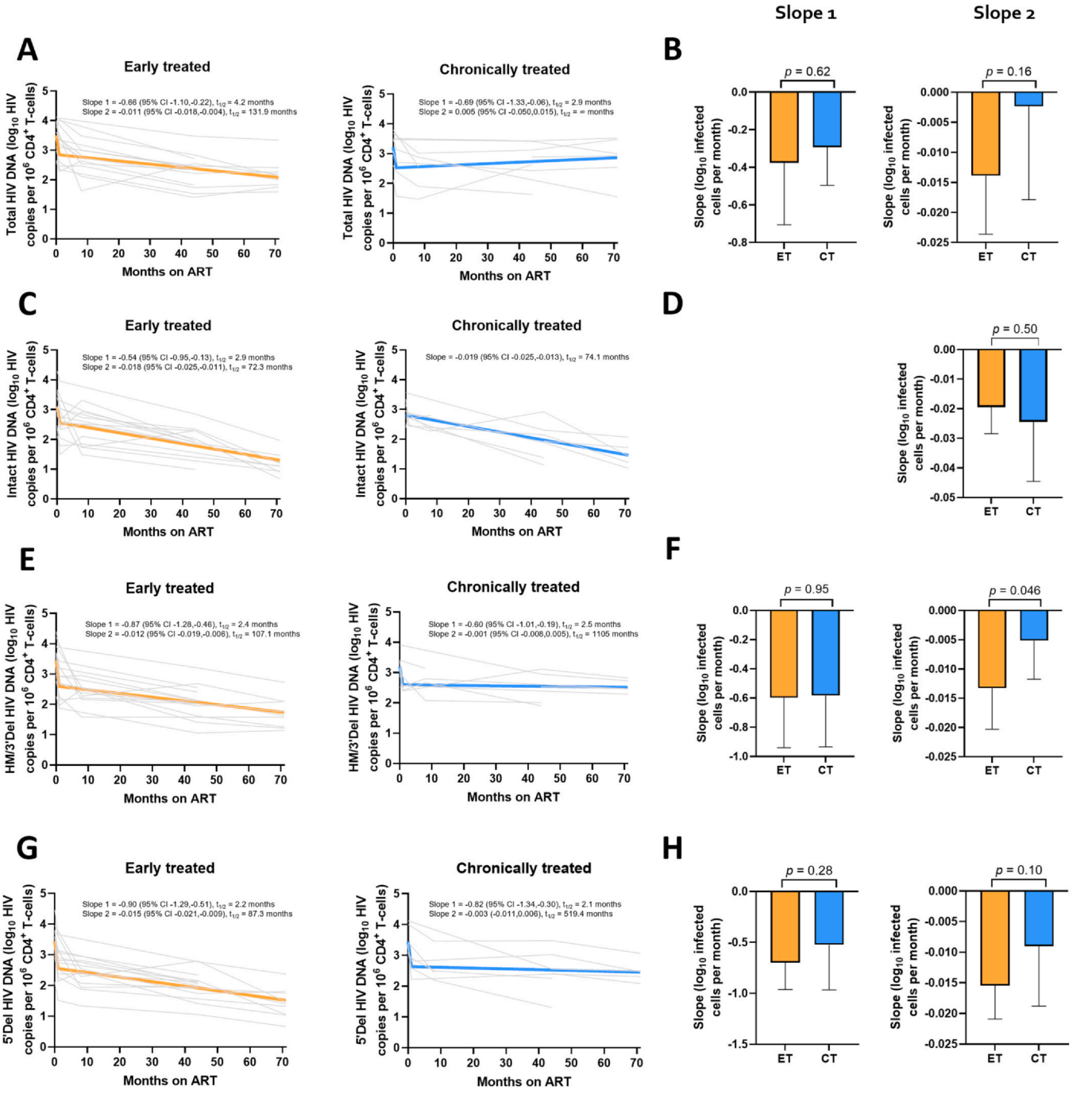

Fig. 1. Evolution of the HIV reservoir over time (longitudinal analysis). Longitudinal dynamics of total HIV DNA (A, B), intact HIV DNA (C, D), and defective HIV DNA, including hypermutated, and/or 3' deleted forms (E, F) and 5' deleted forms (G, H). We used the extra sum-of-squares F test to assess whether the decay of total, intact, and defective HIV DNA was better described by a single-phase linear model or a segmented (two-phase) linear regression model. The best-fitting model is displayed in panels A, C, E, and G. In panels B, D, F, and H, individual slopes for each participant were estimated using linear regression, and the median slope is shown. Differences between the decay slopes were calculated using the Mann-Whitney *U* test. 5'Del, 5' deleted; CT, treated during the chronic phase of infection; ET, early treated; HM/3'Del, hypermutated and/or 3'deleted.

CT, and HNC participants, indicating group-specific metabolic signatures.

In $CD4^+$ T-cells, four metabolites showed nominal differences across the three groups: uric acid, D-fructose, isomaltose, and 4-hydroxyproline (Fig. 4C). In the unadjusted analysis, isomaltose levels were lower in CT compared to ET participants, whereas 4-hydroxyproline was increased in CT participants compared to ET individuals. However, these associations were no longer significant after FDR correction. Random forest analysis identified 4-hydroxyproline as the strongest discriminator between CT and ET participants, while D-fructose most effectively differentiated ET from HNC (Fig. 4D). In $CD8^+$ T-cells, L-glycine was the only metabolite that showing nominal differences across groups. Glycine levels were lower in the ET group compared to HNC and in all HIV+ participants compared to HNC (Fig. 4E), but these differences did not remain significant after FDR correction. Random forest analysis identified L-

Table 2
Demographic and immunovirological characteristics of participants included in the cross-sectional cohort A.

	Early treated (n = 23)	Chronically treated (n = 20)	*p*-value[a]
Age at HIV diagnosis, years	30 (25–40)	33.5 (27.3–44)	0.62
Sex, male	21 (91.3)	17 (85)	0.65
Geographic origin			0.035
Spain	19 (82.6)	13 (65)	
Africa	1 (4.3)	1 (5)	
Central/South America	0 (0)	5 (25)	
Europe (excluding Spain)	1 (4.3)	1 (5)	
HIV-1 subtype			0.27
B	17 (73.9)	10 (50)	
F	2 (8.7)	2 (10)	
G	1 (4.3)	0 (0)	
Recombinant forms	1 (4.3)	2 (10)	
Unknown	2 (8.7)	3 (15)	
Pre-ART HIV-1 VL, copies/mL	481,000 (69,000–6,370,000)	178,000 (81,775–414,750)	0.049
Pre-ART $CD4^+$ T-cell count, cells/μL	450 (330–570)	440 (313–499)	0.64
Nadir $CD4^+$ T-cell count, cells/μL	380 (260–510)	440 (310–499)	0.80
Pre-ART $CD8^+$ T-cell count, cells/μL	805 (610–1252)	912 (679–1115)	0.83
Pre-ART $CD4^+/CD8^+$ ratio	0.55 (0.25–0.72)	0.49 (0.34–0.60)	0.42
Fiebig stage		NA	NA
I	0 (0)		
II	2 (8.7)		
III	3 (13)		
IV	10 (43.5)		
V	4 (17.4)		
VI	4 (17.4)		
First line ART			0.60
INSTI-based	18 (78.3)	14 (70)	
PI-based	3 (13)	2 (10)	
NNRTI-based	2 (8.7)	4 (20)	
Age at inclusion, years	37 (29–51)	42.5 (32.5–51)	0.43
Time on ART an inclusion, months	72 (56–83)	74.5(64–105.3)	0.36
Time virologically suppressed at inclusion, months	65 (48–79)	69.5 (55.5–100.8)	0.37
$CD4^+$ T-cell count at inclusion, cells/μL	610 (530–930)	785 (623–935)	0.28
$CD8^+$ T-cell count at inclusion, cells/μL	690 (540–810)	755 (593–980)	0.29
$CD4^+/CD8^+$ ratio at inclusion	1.05 (0.69–1.58)	1.02 (0.81–1.37)	0.80
ART at inclusion			0.70
INSTI-based	19 (82.6)	15 (75)	
PI-based	0 (0)	1 (5)	
NNRTI-based	4 (17.4)	4 (20)	

Results are expressed as number (%) or median (IQR). ART, antiretroviral therapy; INSTI, integrase strand transfer inhibitor; NA, not applicable; NNRTI, non-nucleoside reverse transcriptase inhibitor; PI, protease inhibitor; VL, viral load.
Percentages may not sum to 100 due to rounding.
[a] *p*-values are the result of the Mann-Whitney *U* test for continuous variables and Fisher's exact test for categorical variables.

glycine and L-isoleucine as effective discriminators between HNC and ET individuals, while D-fructose and pyroglutamic acid best distinguished ET and CT participants (Fig. 4F). Together, these findings suggest that ART timing influences T-cell metabolism in a subset-specific manner, which may have implications for immune function and HIV reservoir dynamics.

Next, we explored potential associations between HIV reservoir parameters and the metabolomic profiles of $CD4^+$ and $CD8^+$ T cells (Fig. 5A and B). We observed positive correlations between CA RNA levels in $CD4^+$ T-cells and several metabolites associated with amino acid metabolism and protein synthesis (L-alanine, L-serine, L-threonine, and the branched-chain amino acids L-leucine, L-isoleucine and L-valine), as well as other amino acid-derived metabolites (ornithine and N-acetylglycine)[35]; glutathione metabolism (pyroglutamic acid)[36,37]; membrane lipid synthesis (ethanolamine)[38]; and energy metabolism, including glycolysis (D-fructose and—indirectly via glycerate intermediates—glyceric acid),[39] the Krebs cycle (citric acid),[40] and the polyol pathway (D-sorbitol).[41] These correlations were more pronounced in the CT group than in ET participants (Fig. 5A), particularly in the case of ethanolamine, L-leucine, L-isoleucine, N-acetylglycine, pyroglutamic acid, D-sorbitol, and sucrose (Fig. 5C). Despite these correlations, there were no significant differences in the levels of these metabolites between groups (Fig. 5D). In contrast, in $CD8^+$ T-cells, we did not observe strong positive correlations between HIV reservoir measures and metabolites. However, some metabolites linked to branched-chain amino acid catabolism (such as 2-hydroxyisobutyric acid and 2-ketoisocaproic acid) were negatively correlated with CA RNA levels (Fig. 5B).

Collectively, these findings suggest that $CD4^+$ T-cell metabolism, particularly amino acid and energy pathways, may play a key role in sustaining HIV transcriptional activity, with more pronounced effects in participants with late ART initiation.

Discussion

Strategies that can limit the size of the viral reservoir, such as early ART during AHI, are paramount to developing HIV cure strategies. Here, we present longitudinal analyses of viral reservoir decay, coupled with plasma cytokine profiling and T-cell metabolomic data, revealing how early versus late ART initiation influences both the size and composition of the reservoir, as well as associated immunometabolic pathways.

In consonance with previous reports,[10,11] the longitudinal decay of total HIV DNA was more pronounced in the ET group and followed a biphasic model. After a median of 69 months of ART-induced virological suppression, we observed that the size of the total HIV

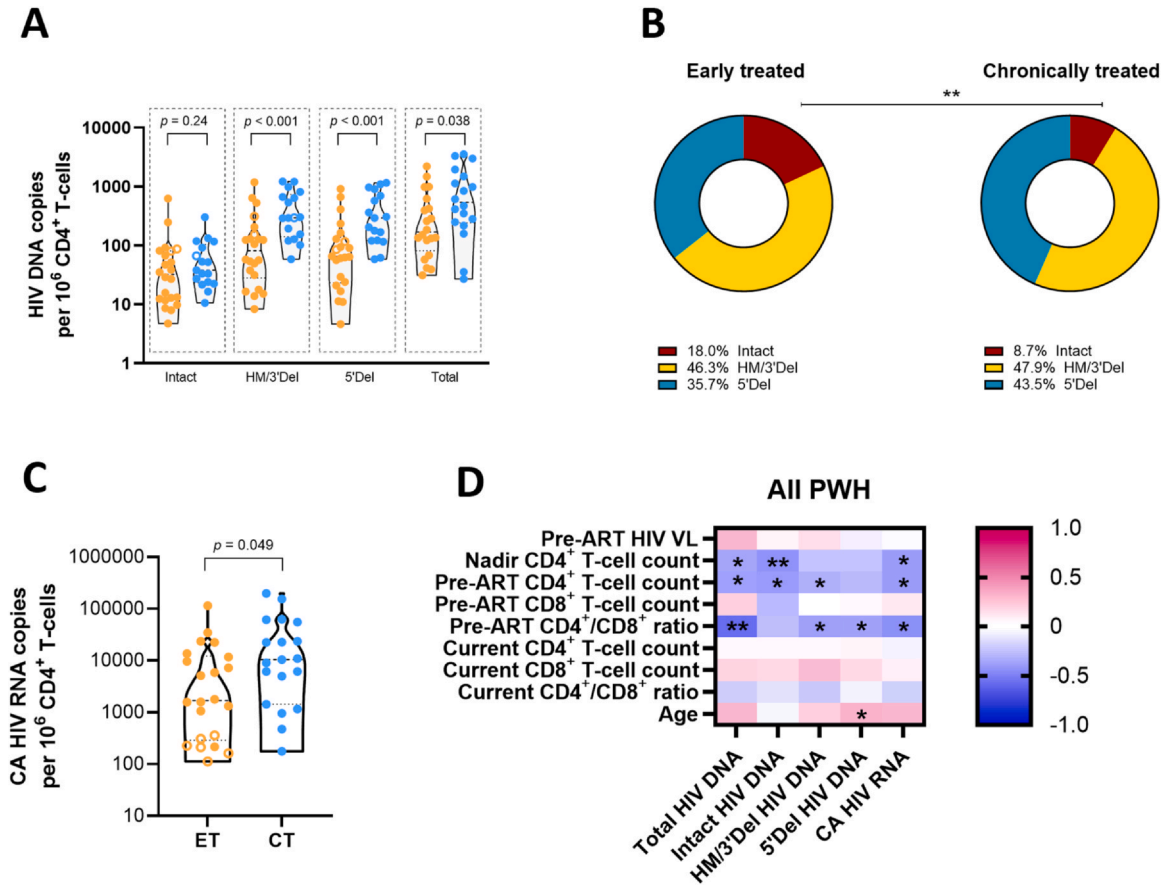

Fig. 2. Cross-sectional reservoir analysis. (A) Comparison of total, intact, and defective HIV DNA between ET and CT participants. (B) Proportion of intact and defective proviruses relative to the total HIV reservoir in ET and CT individuals. (C) Cell-associated (CA) HIV RNA in ET and CT participants. (D) Heatmap showing correlations between demographic and immunological parameters and HIV reservoir measures. Blue circles represent CT participants and orange circles represent ET participants. Open circles indicate values below the limit of detection. Total HIV DNA by qPCR failed to amplify in 3 ET and 2 CT participants. IPDA assay failed to amplify in 1 ET and 3 CT participants. CA HIV RNA by qPCR failed to amplify in 1 ET and 1 CT participant. 5'Del, 5' deleted; CA, cell-associated; CT, treated during the chronic phase of infection; ET, early treated; HM/3'Del, hypermutated and/or 3'deleted; PWH, people with HIV. *p*-values were calculated using the Mann-Whitney *U* test in panels A–C and Spearman's correlation test in panel D. In panel D, only statistically significant correlations ($p < 0.05$) are shown. *: $p < 0.05$, **: $p < 0.01$. Percentages may not sum to 100 due to rounding.

reservoir was reduced in ET compared to CT participants, consistent with findings from earlier studies.[11,12,42,43]

Regarding the surrogate of the replication-competent reservoir, we observed similar levels of intact HIV DNA after prolonged (≥3 years) ART-induced virological suppression among PWH who had comparable pre-ART immunological profiles (median 440 $CD4^+$ T-cells/μL and $CD4^+/CD8^+$ ratio of 0.51) and started early (< 180 days since HIV acquisition) or late ART (≥180 days). Recently, Gandhi et al. also reported similar levels of intact proviruses after 2 and 4–6 years of ART in ET and CT PWH.[44] In our study, although absolute intact HIV DNA levels did not differ between groups, the proportion of intact proviruses relative to the total HIV reservoir was higher in ET participants (18%) than in CT individuals (9%), which aligns with previous reports describing the accumulation of defective proviruses with late ART initiation.[45,46]

While the decay pattern of intact proviruses differed between ET participants and CT participants (a two-phase model with a steeper initial decline versus a one-phase linear model, respectively), the decay rate of intact proviruses beyond the initial phase was similar between the two groups. Similarly, Gandhi et al. described a continuous decay of intact proviruses in both ET and CT individuals after 2 years of ART, without significant differences between groups.[44] These results contrast with a previous study,[12] which found a faster decay of intact proviruses among very early treated participants (88% diagnosed at Fiebig stage I) compared to those treated during chronic HIV infection. In our study, most individuals in the longitudinal ET group were diagnosed at Fiebig stages IV–VI (none at Fiebig stage I, and only 3 out of 14 at Fiebig stages II–III). Massanella et al. also reported an increased decline of the inducible HIV reservoir (measured by tat/rev induced limiting dilution assay) in ET participants, but time from EDI to the start of ART was much shorter than in our cohort (21 versus 46 days in our longitudinal analysis and 73 days in our cross-sectional analysis).[10] These differences in the timing of ART initiation might explain the discrepancies in intact HIV DNA decay patterns between cohorts. As HIV rapidly disseminates throughout the body in the very first days of infection,[47] it is possible that only prompt ART during the earliest Fiebig stages can impact the intact viral reservoir. However, this raises the question of whether we can realistically expect to significantly influence the intact reservoir with early ART, since diagnosing HIV infection and starting ART at Fiebig stages I or II (before the onset of symptoms and with negative serologic tests) can be difficult to achieve in real-world clinical scenarios.

In contrast with the continuous decay of intact proviruses in both cohorts, defective proviruses showed a persistent decline in ET participants but plateaued in CT individuals after an initial phase of steep decline. These findings are consistent with previous studies

Table 3
Demographic and immunovirological characteristics of participants included in the matched cross-sectional cohort B.

	Early treated (n = 13)	Chronically treated (n = 13)	HIV-negative controls (n = 13)	*p*-value[a]
Age at HIV diagnosis, years	30 (25.5–45.5)	27.5 (23–36.5)	NA	0.96
Sex, male	12 (92.3)	12 (92.3)	12 (92.3)	1.00
Geographic origin				0.84
Spain	12 (92.3)	10 (76.9)	12 (92.3)	
Africa	1 (7.7)	1 (7.7)	1 (7.7)	
Central/South America	0 (0)	1 (7.7)	0 (0)	
Europe (excluding Spain)	0 (0)	1 (7.7)	0 (0)	
HIV-1 subtype			NA	0.40
B	8 (61.5)	8 (61.5)		
F	2 (15.4)	0 (0)		
G	1 (7.7)	0 (0)		
Recombinant forms	0 (0)	2 (15.4)		
Unknown	2 (15.4)	3 (15.4)		
Pre-ART HIV-1 VL, copies/mL	365,000 (50,000–3,771,603)	270,000 (87,000–674,000)	NA	0.42
Pre-ART CD4$^+$ T-cell count, cells/μL	420 (294–495)	440 (290–500)	NA	0.72
Nadir CD4$^+$ T-cell count, cells/μL	340 (259–445)	440 (290–500)	NA	0.17
Pre-ART CD8$^+$ T-cell count, cells/μL	715 (558–1268)	912 (590–1060)	NA	0.94
Pre-ART CD4$^+$/CD8$^+$ ratio	0.54 (0.22–0.74)	0.50 (0.41–0.59)	NA	0.77
Fiebig stage		NA	NA	NA
I	0 (0)			
II	1 (7.1)			
III	2 (15.4)			
IV	7 (53.8)			
V	1 (7.7)			
VI	2 (15.4)			
First line ART			NA	0.75
INSTI-based	8 (61.5)	7 (53.8)		
PI-based	3 (32.1)	2 (15.4)		
NNRTI-based	2 (15.4)	4 (30.8)		
Age at inclusion, years	40 (32–52.5)	41 (34–52)	41 (30.5–52.5)	0.98
Time on ART an inclusion, months	73 (61.5–105)	87 (64–118)	NA	0.48
Time virologically suppressed at inclusion, months	72 (59–101)	79 (57.5–114)	NA	0.48
CD4$^+$ T-cell count at inclusion, cells/μL	580 (515–885)	800 (700–975)	NA	0.091
CD8$^+$ T-cell count at inclusion, cells/μL	690 (425–780)	770 (650–960)	NA	0.17
CD4$^+$/CD8$^+$ ratio at inclusion	1.03 (0.76–1.70)	1.02 (0.86–1.32)	NA	1.00
ART at inclusion			NA	1.00
INSTI-based	10 (76.9)	10 (76.9)		
PI-based	0 (0)	0 (0)		
NNRTI-based	3 (23.1)	3 (23.1)		

Results are expressed as number (%) or median (IQR). ART, antiretroviral therapy; INSTI, integrase strand transfer inhibitor; NA, not applicable; NNRTI, non-nucleoside reverse transcriptase inhibitor; PI, protease inhibitor; VL, viral load.
Percentages may not sum to 100 due to rounding.
[a] *p*-values are the result of the Mann-Whitney *U* test for continuous variables when comparing 2 groups, Kruskal-Wallis test for continuous variables when comparing > 2 groups, and Fisher's exact test for categorical variables.

describing a much slower decline of defective versus intact proviruses,[15] and stabilization of defective proviral DNA levels over time[14,16,44] in participants treated during chronic HIV infection.

A recent analysis of our AHI cohort suggests that pre-ART CD4$^+$/CD8$^+$ ratio, an indirect marker of preserved immune function, may be a better predictor of CD4$^+$/CD8$^+$ ratio normalization than very early ART initiation (within the first 30 days after HIV acquisition).[31] Likewise, preserved pre-ART immunological status has been linked to accelerated reservoir clearance, as participants in a cohort of acutely treated PWH who started ART with higher CD4$^+$ T-cell counts exhibited faster decay of both intact and defective HIV DNA.[13] In line with these results, in our cross-sectional analysis, participants with a pre-ART CD4$^+$/CD8$^+$ ratio < 0.5 had significantly higher total HIV DNA and CA HIV RNA levels, and both pre-ART CD4$^+$/CD8$^+$ ratio and pre-ART CD4+ T-cell counts were negatively correlated with total reservoir size and HIV transcription.

In our study, we did not find significant differences in plasma cytokine levels between ET and CT participants after correction for multiple testing. However, IL-10 was higher in ET participants than in CT individuals and HNC in the unadjusted analysis. In addition, only IL-10, MMP-1, and MIG were nominally increased in PWH compared to HNC, but these differences did not persist after FDR correction. IL-10, an anti-inflammatory cytokine, has been linked to persistent viral infections, including HIV,[48,49] and to impaired HIV specific immunity.[50] MMP-1, an interstitial collagenase, degrades extracellular matrix components and contributes to tissue homeostasis by regulating extracellular tissue signaling networks.[51] MIG is a chemokine that regulates immune cell migration,[52] and has previously been reported to be upregulated in PWH.[53]

Although previous studies have reported attenuated inflammation in participants treated during AHI,[21–25] they either lacked a comparison with participants treated during chronic HIV infection[22] or HIV-negative controls,[23,25] or only provided short-term data (after 6–24 months on ART).[21–24] Moreover, considerable heterogeneity exists between studies, as each assesses different classes of biomarkers. To the best of our knowledge, this is the first study to report a longer-term comparison of inflammatory markers between ET and CT PWH. Participants in our study were virologically suppressed for a median of 74 months, which is longer than in previous studies and may partly explain differences from previous reports. However, given the small sample size (13 participants per group) and the large number of analytes assessed, our study may be underpowered to detect modest between-group differences. Therefore, our findings should be considered exploratory and interpreted with caution.

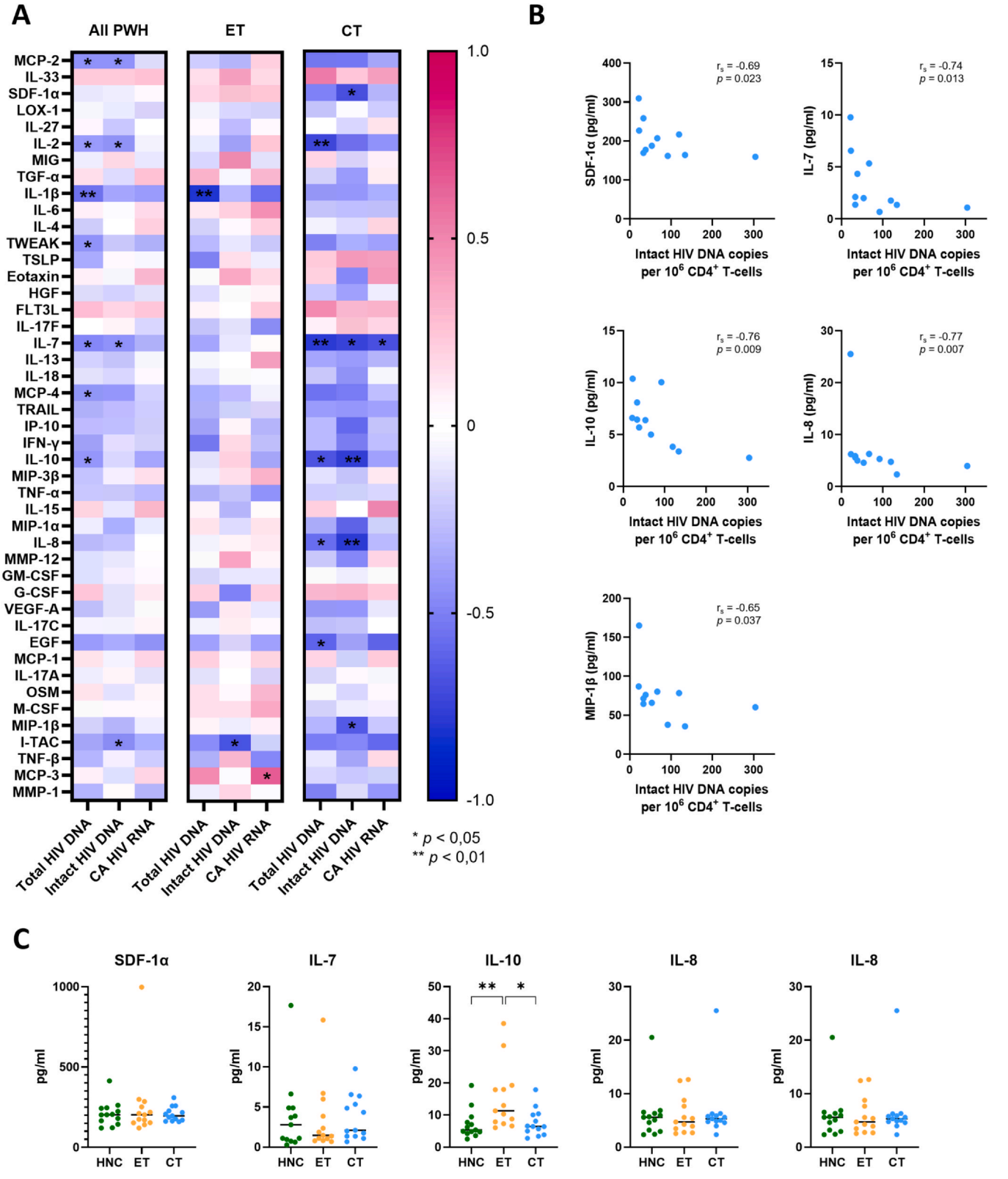

Fig. 3. Plasma cytokines. (A) Heatmap showing Spearman's rank correlation coefficients between plasma cytokine levels and HIV reservoir measures. Color intensity indicates the strength and direction of correlation. (B) Scatter plots of Spearman's rank correlations between intact HIV DNA and selected cytokines identified in panel A in CT participants. Each dot represents one participant. Spearman's rank correlation coefficient and corresponding *p*-value are shown in each panel. (C) Comparison of selected cytokine levels across participant groups: HIV-negative controls, early treated participants, and participants treated during the chronic phase of infection (green, orange, and blue, respectively). Each dot represents one participant, and horizontal bars indicate the median. Comparisons were performed using the Kruskal-Wallis test followed by post-hoc Dunn's multiple comparisons test, and unadjusted *p*-values are shown. Asterisks denote statistically significant correlations (panel A) or unadjusted group differences (panel C). *: $p < 0.05$, **: $p < 0.01$. In panel C, no differences remained statistically significant after FDR correction. CA, cell-associated; CT, treated during the chronic phase of infection; ET, early treated; HNC, HIV-negative controls; PWH, people with HIV, r_s, Spearman's rank correlation coefficient.

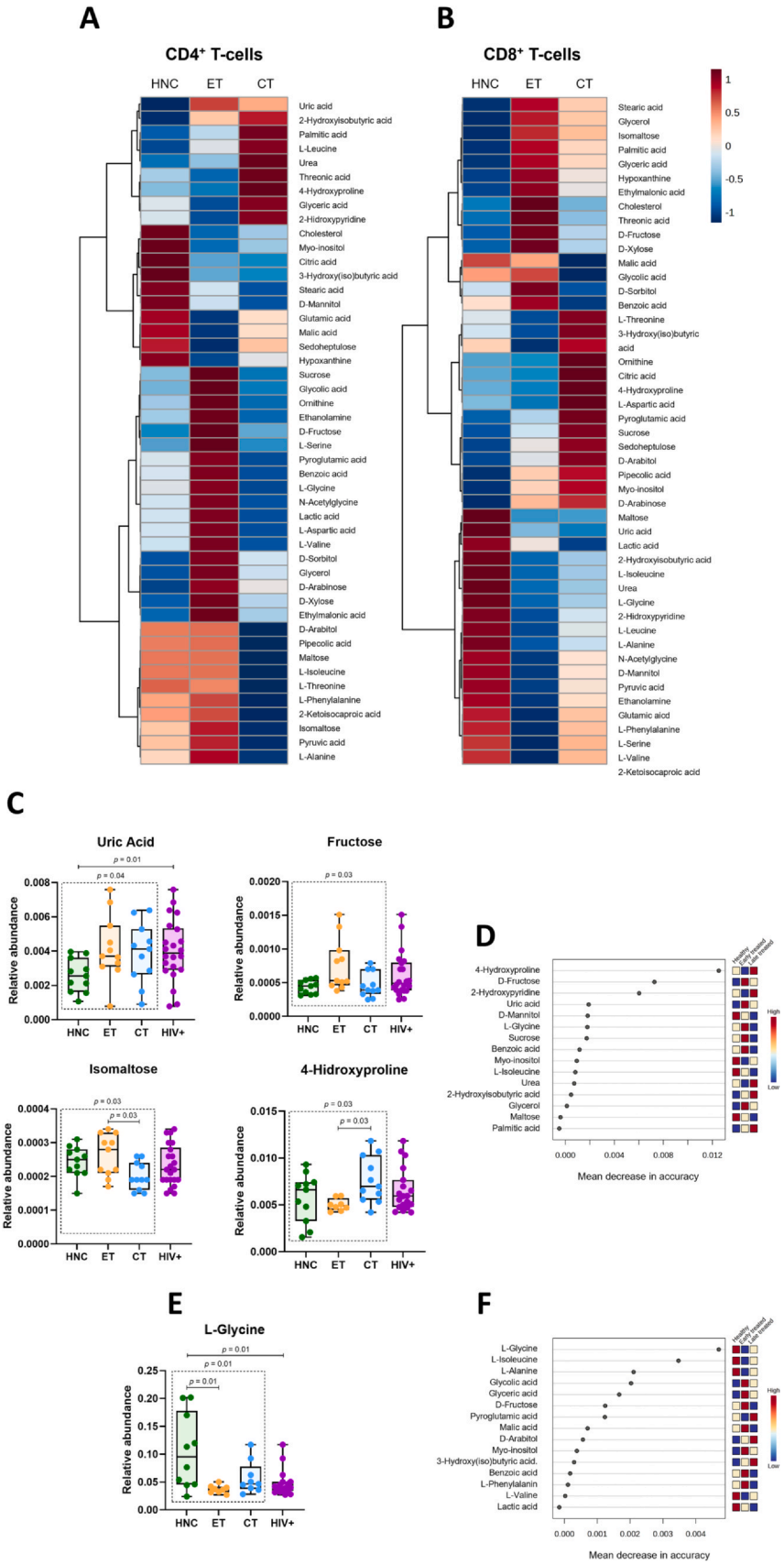

(caption on next page)

Fig. 4. Metabolomic profiles of CD4⁺ and CD8⁺ T-cells. (A-B) Heatmaps showing the relative abundance of metabolites in (A) CD4⁺ and (B) CD8⁺ T-cells across groups: HIV-negative controls (HNC), early treated (ET) participants, and participants treated during the chronic phase of infection (CT). Color intensity indicates relative metabolite abundance. (C, E) Comparison of selected metabolites that significantly differed between groups in (C) CD4⁺ and (E) CD8⁺ T-cells. Green represents HNC, orange represents ET participants, blue represents CT participants, and purple represents all HIV+ participants. Each dot represents one participant. Group differences between HNC, ET, and CT groups were assessed using the Kruskal-Wallis test followed by post-hoc Dunn's multiple comparisons test. Group differences between HNC and all HIV+ participants were assessed using the Mann-Whitney *U* test. Statistical comparisons are shown using unadjusted *p*-values. FDR correction was applied separately to Kruskal-Wallis and Mann-Whitney analyses; no metabolites remained statistically significant after correction. (D, F) Random forest analysis identifying the top metabolites discriminating between groups in (D) CD4⁺ and (F) CD8⁺ T-cells. Metabolites are ranked by mean decrease in accuracy. Side heatmaps show the relative abundance of each metabolite across study groups.

Differences in the biomarkers analysed across studies also limit direct comparability with our results, as we measured circulating cytokines and chemokines, whereas other studies have also assessed acute-phase proteins and markers of monocyte activation, microbial translocation, or coagulation.[21–25]

Importantly, despite scarce differences in plasma cytokine concentrations across groups, we observed significant negative correlations between several pro-inflammatory, homeostatic, and anti-inflammatory cytokines (including IL-10) and intact HIV DNA in CT participants. A recent study also described an association between higher levels of IL-10 during ART-induced viral suppression and lower levels of intact HIV DNA.[54] Altogether, these findings suggest that, beyond overt systemic inflammation, alterations in the complex cytokine networks regulating immune activation and inflammation persist despite ART. These alterations in the cytokine milieu seem to correlate more strongly with the intact HIV reservoir in CT individuals, potentially through effects on CD4⁺ T-cell survival, homeostasis, and activation.

The role of cellular metabolism in the establishment and dynamics of viral reservoirs remains poorly understood. Characterizing the metabolic profiles of CD4⁺ and CD8⁺ T-cells, and the differences associated with early versus late ART, can provide valuable insights into HIV pathogenesis. Nevertheless, we did not assess T-cell functional or phenotypic markers in this cohort, and therefore the biological interpretation of these metabolic associations should be considered speculative. Our results suggest that ART timing is associated with distinct metabolic signatures in both CD4⁺ and CD8⁺ T-cells. CD4⁺ T-cells exhibited more pronounced differences between ET and CT participants in the unadjusted analysis, particularly for 4-hydroxyproline and isomaltose. Although these differences did not survive FDR correction, these exploratory findings may be indicative of early ART preserving specific metabolic pathways in this subset of T-cells. Reduced isomaltose levels in the CT group may reflect alterations in sugar metabolism, which have been previously associated with impaired CD4⁺ T-cell functionality.[55] Hydroxyproline is a non-essential amino acid formed by the post-translational hydroxylation of proline, and contributes to the stabilization of collagen structure.[56] CD4⁺ T-cell 4-hydroxyproline levels were nominally higher in CT participants than in the ET group, representing the strongest differentiating metabolite between the two groups. High hydroxyproline levels can induce programmed death-ligand 1 (PD-L1) expression depending on IFN-γ.[57] In the context of HIV infection, PD-L1 has been linked to impaired HIV-specific T helper responses, and its blockade may enhance effector functions of T helper cells.[58] Increased 4-hydroxyproline might therefore signal CD4⁺ T-cell dysfunction in CT PWH. Lower levels in the ET group may reflect enhanced T helper cell response when ART is started during AHI.

In CD8⁺ T-cells, only glycine levels were higher in HNC than in HIV+ participants in the unadjusted analysis, without differences between ET and CT groups or after FDR correction. Glycine is a non-essential amino acid involved in protein synthesis and mitochondrial function. In PWH, the mitochondrial enzyme SHMT2 (responsible for converting serine to glycine) is downregulated in CD8⁺ T-cells.[59] This reduced expression may account for the decreased glycine levels observed in PWH compared to HNC. Interestingly, in vitro glycine supplementation has been reported to improve mitochondrial function and attenuate cellular senescence in CD8⁺ T-cells,[59] highlighting its potential therapeutic relevance.

In our cohort, several metabolites that have been previously described as being involved in various metabolic pathways, such as amino acid metabolism, glutathione metabolism, membrane lipid synthesis, and energy metabolism exhibited strong positive correlations with HIV transcription in CD4⁺ T-cells, particularly in CT participants. Specifically, branched-chain amino acids such as leucine and isoleucine activate the mTOR signaling pathway,[60] which has been linked to regulation of HIV latency[61]; ethanolamine is a precursor of phosphatidylethanolamine, a phospholipid involved in membrane composition,[38] and may relate to viral assembly and budding[62]; and sorbitol participates in the polyol pathway,[41] suggesting possible alterations in cellular energy metabolism that could be consistent with metabolic reprogramming of activated CD4⁺ T-cells. Together, these alterations may reflect a cellular environment that is permissive to HIV transcription in CD4⁺ T-cells in CT individuals. The metabolic environment of CD8⁺ T-cells appeared to be less altered, consistent with CD4⁺ T-cells being a primary target of persistent HIV infection. Importantly, these associations are correlative and should be interpreted as hypothesis-generating.

Our study has several limitations. First, the sample size was small. Second, CT participants in the longitudinal analysis were not matched to ET participants. Third, the exclusion of ET participants without a suitable matched CT control reduced the sample size of the matched cross-sectional cohort B and may have introduced selection bias. However, included and excluded ET participants were comparable across baseline clinical and immunovirological parameters (Table S2). Moreover, confounding factors may have influenced some of the observed associations, as ART timing, pre-ART CD4⁺/CD8⁺ ratio, age, inflammation, and metabolic alterations might be interconnected and related to unmeasured parameters such as microbial translocation. We did not perform multivariate analyses due to the limited sample size.

Additionally, HIV-1 subtype diversity may have influenced IPDA performance, although amplification failure was not restricted to non-B subtypes and occurred in only 2 of 16 participants with non-B or unknown subtypes. While nominal differences in cytokines and metabolites were identified, these associations did not withstand correction for multiple testing and should therefore be considered exploratory and interpreted in the context of limited statistical power due to the small sample size. Finally, we did not evaluate T-cell functional or phenotypic markers, which limits the mechanistic interpretation of our findings.

Nonetheless, the study also has important strengths. To the best of our knowledge, this is the first cross-sectional study to match ET and CT participants by key clinical and immunovirological variables to minimize biases from heterogenous pre-ART immunological status or varying ART duration that could influence reservoir size or inflammatory markers. Furthermore, our study combines measures of the viral reservoir, plasma inflammatory activity, and metabolic profiling of T-cells to provide a comprehensive view of the multifaceted effects of initiating ART during AHI.

In conclusion, our results suggest that, although early ART can impact the total and defective viral reservoir, it might not be enough to reduce the intact HIV reservoir or prevent metabolic alterations in T-cells. In CT participants, alterations in the cytokine milieu and the CD4⁺ T-cell metabolic landscape correlate with the replication competent reservoir and HIV transcription, suggesting that the

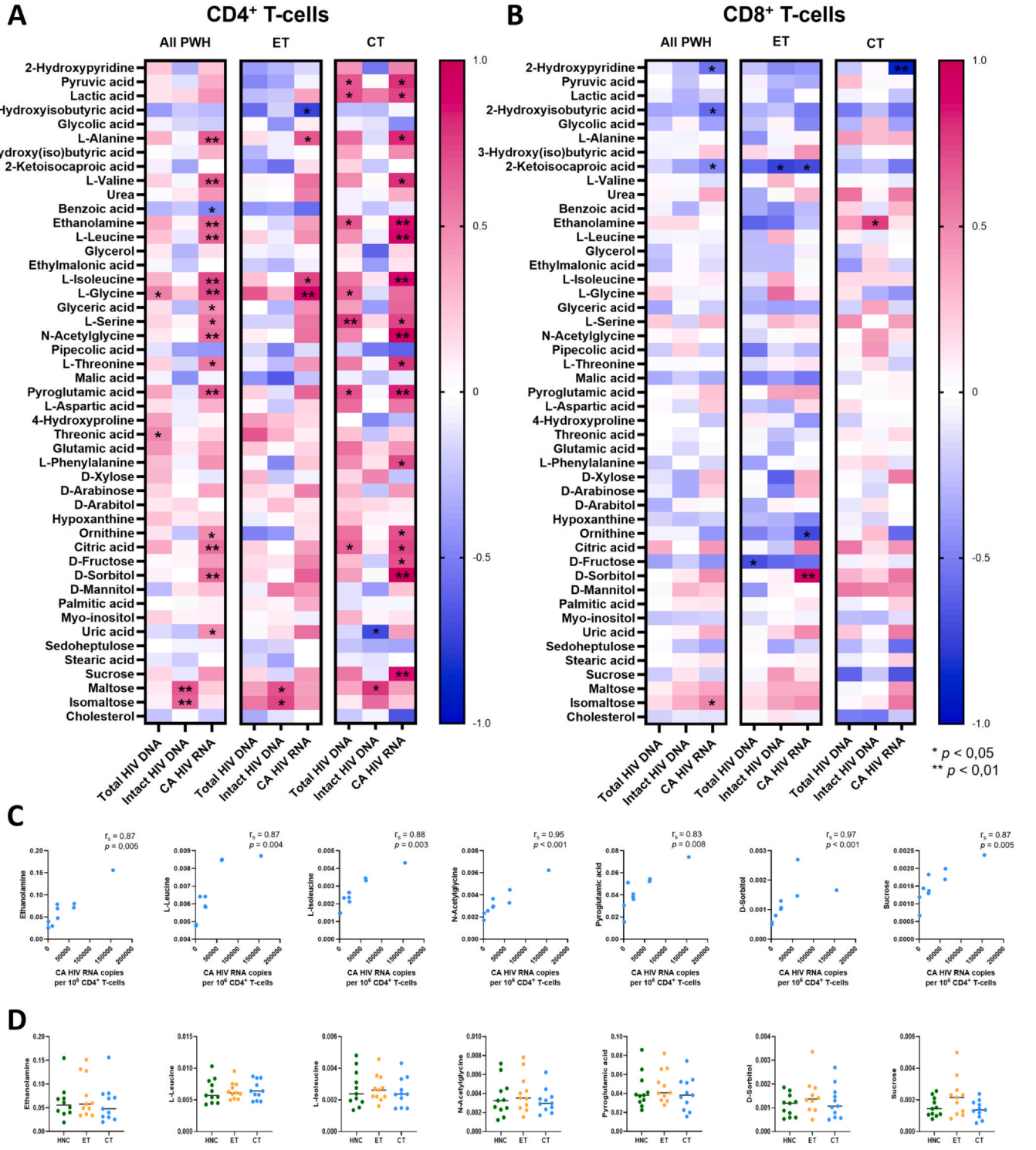

Fig. 5. Correlations between metabolites and HIV reservoir measures. (A-B) Heatmaps showing Spearman's rank correlation coefficients between HIV reservoir measures and metabolites in (A) $CD4^+$ and (B) $CD8^+$ T-cells. Color intensity indicates the strength and direction of correlation. Asterisks denote statistically significant correlations (*: $p < 0.05$, **: $p < 0.01$). (C) Scatter plots of Spearman's rank correlations between CA HIV RNA and selected metabolites in $CD4^+$ T-cells identified in panel A in CT participants. Each dot represents one participant. Spearman's rank correlation coefficient and corresponding p-value are shown in each panel. (D) Comparison of selected metabolite levels in $CD4^+$ T-cells across participant groups: HIV-negative controls, early treated participants, and participants treated during the chronic phase of infection (green, orange, and blue, respectively). Each dot represents one participant, and horizontal bars indicate the median. Comparisons were performed using the Kruskal-Wallis test followed by post-hoc Dunn's multiple comparisons test (p-values are not shown as all were > 0.05). CA, cell-associated; CT, treated during the chronic phase of infection; ET, early treated; PWH, people with HIV; r_s, Spearman's rank correlation coefficient.

timing of ART may influence immune and metabolic pathways related to HIV persistence. Whether these persistent alterations are associated with T-cell function or influence clinical outcomes remains to be explored. Larger studies including participants with well-matched immunovirological and clinical characteristics are needed to better understand the effect of ART during the early phases of HIV infection, and to determine the implications of these findings for HIV cure strategies.

Author contributions

PS, JN, VF, and MJB designed the study. PS, JN, PAL, VD, JNG, AM, AC, JB, and VF selected the participants. PS collected the data. JGE performed the experiments. All authors contributed to data analysis and interpretation. PS drafted the manuscript, which was critically revised and amended by JGE, JN, SC, AR, ARS, PAL, VD, JNG, AM, AC, JB, BP, MS, MG, VF, and MJB. PS and JGE contributed equally to this work. All authors read and approved the final version of the manuscript.

Funding

This study was funded by the Instituto de Salud Carlos III through project PI20/00823 (co-funded by the European Regional Development Fund/European Social Fund; “A way to make Europe”/ "Investing in your future". This study was also supported by the Spanish Network for AIDS Research (RIS), which is funded through the Instituto de Salud Carlos III – Red Temática de Investigación Cooperativa en Sida (RD06/006, RD12/0017/0018 and RD16/0002/0006) as part of the Plan Nacional de I+D+I, and co-financed by the Instituto de Salud Carlos III-Subdirección General de Evaluación and the Fondo Europeo de Desarrollo Regional (FEDER). For this project, PS has received a grant from the Catalan Society of Infectious Diseases and Clinical Microbiology (SCMIMC) funded by ViiV Healthcare. MJB is supported by the Miguel Servet program funded by the Spanish Health Institute Carlos III (CPII22/00005). The funders had no role in the study design, data collection and interpretation, or the decision to submit the work for publication.

Declaration of Competing Interest

The authors declare the following financial interests/personal relationships which may be considered as potential competing interests: PS has received honoraria and/or speaking fees and/or financial support for attending conferences from Gilead, Janssen-Cilag, Merck Sharp & Dome, Pfizer, and ViiV Healthcare outside of the submitted work. JN has as received honoraria and/or speaking fees and/or financial support for attending conferences from Abbvie, Gilead, Janssen-Cilag, Merck Sharp & Dome, and ViiV Healthcare outside of the submitted work. AC, AM, JB, JNG, PA, and VF have received honoraria and/or speaking fees and/or financial support for attending conferences from Gilead, Janssen-Cilag, Merck Sharp & Dome and ViiV Healthcare outside of the submitted work. VD has received honoraria and/or speaking fees and/or financial support for attending conferences from Gilead, Merck Sharp & Dome and ViiV Healthcare outside of the submitted work. The remaining authors declare no conflicts of interest.

Appendix A. Supplementary material

Supplementary data associated with this article can be found in the online version at doi:10.1016/j.jinf.2026.106754.

References

1. Palella FJ, Delaney KM, Moorman AC, Loveless MO, Fuhrer J, Satten GA, et al. *Declining morbidity and mortality among patients with advanced human immunodeficiency virus infection. N Engl J Med* 1998;**338**:853–60. https://doi.org/10.1056/NEJM199803263381301
2. Tusch E, Ryom L, Pelchen-Matthews A, Mocroft A, Elbirt D, Oprea C, et al. *Trends in mortality in people with HIV from 1999 through 2020: a multicohort collaboration. Clin Infect Dis* 2024;**79**(5):1242–57. https://doi.org/10.1093/cid/ciae228. PubMed PMID: 38663013.
3. Trickey A, Sabin CA, Burkholder G, Crane H, d'Arminio Monforte A, Egger M, et al. *Life expectancy after 2015 of adults with HIV on long-term antiretroviral therapy in Europe and North America: a collaborative analysis of cohort studies. Lancet HIV* 2023;**10**(5):e295–307. https://doi.org/10.1016/S2352-3018(23)00028-0. PubMed PMID: 36958365.
4. Nance RM, Chris Delaney JA, Simoni JM, Wilson IB, Mayer KH, Whitney BM, et al. *HIV viral suppression trends over time among HIV-infected patients receiving care in the United States, 1997 to 2015 a cohort study. Ann Intern Med* 2018;**169**(6):376–84. https://doi.org/10.7326/M17-2242. PubMed PMID: 30140916.
5. Karim SSA, Karim QA. *Antiretroviral prophylaxis: a defining moment in HIV control. Lancet* 2011;**378**:e23–5. https://doi.org/10.1016/S0140
6. McMyn NF, Varriale J, Fray EJ, Zitzmann C, MacLeod H, Lai J, et al. *The latent reservoir of inducible, infectious HIV-1 does not decrease despite decades of antiretroviral therapy. J Clin Investig* 2023;**133**(17):e171554. https://doi.org/10.1172/JCI171554. PubMed PMID: 37463049.
7. Chun TW, Engel D, Berrey MM, Shea T, Corey L, Fauci AS. *Early establishment of a pool of latently infected, resting CD4+ T cells during primary HIV-1 infection. Proc Natl Acad Sci USA* 1998;**95**(15):8869–73. https://doi.org/10.1073/pnas.95.15.8869. PubMed PMID: 9671771.
8. Ananworanich J, Schuetz A, Vandergeeten C, Sereti I, de Souza M, Rerknimitr R, et al. *Impact of multi-targeted antiretroviral treatment on gut T cell depletion and HIV reservoir seeding during acute HIV infection. PLoS One* 2012;**7**(3):e33948. https://doi.org/10.1371/journal.pone.0033948. PubMed PMID: 22479485.
9. Pankau MD, Reeves DB, Harkins E, Ronen K, Jaoko W, Mandaliya K, et al. *Dynamics of HIV DNA reservoir seeding in a cohort of superinfected Kenyan women. PLoS Pathog* 2020;**16**(2):e1008286. https://doi.org/10.1371/journal.ppat.1008286. PubMed PMID: 32023326.
10. Massanella M, Bender Ignacio RA, Lama JR, Pagliuzza A, Dasgupta S, Alfaro R, et al. *Long-term effects of early antiretroviral initiation on HIV reservoir markers: a longitudinal analysis of the MERLIN clinical study. Lancet Microbe* 2021;**2**(5):e198–209. https://doi.org/10.1016/S2666-5247(21)00010-0
11. Buzon MJ, Martin-Gayo E, Pereyra F, Ouyang Z, Sun H, Li JZ, et al. *Long-term antiretroviral treatment initiated at primary HIV-1 infection affects the size, composition, and decay kinetics of the reservoir of HIV-1-infected CD4 T cells. J Virol* 2014;**88**(17):10056–65. https://doi.org/10.1128/jvi.01046-14. PubMed PMID: 24965451.
12. Reddy K, Lee GQ, Reddy N, Chikowore TJ, Baisley K, Dong KL, et al. *Differences in HIV-1 reservoir size, landscape characteristics, and decay dynamics in acute and chronic treated HIV-1 Clade C infection. eLife* 2025;**13**:RP96617. https://doi.org/10.7554/eLife
13. Barbehenn A, Shi L, Shao J, Hoh R, Hartig HM, Pae V, et al. *Rapid biphasic decay of intact and defective HIV DNA reservoir during acute treated HIV disease. Nat Commun* 2024;**15**(1):9966. https://doi.org/10.1038/s41467-024-54116-1. PubMed PMID: 39557853.
14. Gandhi RT, Cyktor JC, Bosch RJ, Mar H, Laird GM, Martin A, et al. *Selective decay of intact HIV-1 proviral DNA on antiretroviral therapy. J Infect Dis* 2021;**223**(2):225–33. https://doi.org/10.1093/infdis/jiaa532. PubMed PMID: 32823274.
15. Peluso MJ, Bacchetti P, Ritter KD, Beg S, Lai J, Martin JN, et al. *Differential decay of intact and defective proviral DNA in HIV-1–infected individuals on suppressive antiretroviral therapy. JCI Insight* 2020;**5**(4):e132997. https://doi.org/10.1172/jci.insight.132997. PubMed PMID: 32045386.
16. Nühn MM, Bosman K, Huisman T, Staring WHA, Gharu L, De Jong D, et al. *Selective decline of intact HIV reservoirs during the first decade of ART followed by stabilization in memory T cell subsets. AIDS* 2025;**39**(7):798–811. https://doi.org/10.1097/QAD.0000000000004160. PubMed PMID: 39964317.
17. Neuhaus J, Jacobs DR, Baker JV, Calmy A, Duprez D, Rosa ALa, et al. *Markers of inflammation, coagulation, and renal function are elevated in adults with HIV infection. J Infect Dis* 2010;**201**(12):1788–95. https://doi.org/10.1086/652749. PubMed PMID: 20446848.
18. Wada NI, Jacobson LP, Margolick JB, Breen EC, Macatangay B, Penugonda S, et al. *The effect of HAART-induced HIV suppression on circulating markers of inflammation and immune activation. AIDS* 2015;**29**(4):463–71. https://doi.org/10.1097/QAD.0000000000000545. PubMed PMID: 25630041.
19. Bloch M, John M, Smith D, Rasmussen TA, Wright E. *Managing HIV-associated inflammation and ageing in the era of modern ART. HIV Med* 2020;**21**(S3):2–16. https://doi.org/10.1111/hiv.12952. PubMed PMID: 33022087.
20. Zicari S, Sessa L, Cotugno N, Ruggiero A, Morrocchi E, Concato C, et al. *Immune activation, inflammation, and non-AIDS co-morbidities in HIV-infected patients under long-term ART. Viruses* 2019;**11**(3):200. https://doi.org/10.3390/v11030200. PubMed PMID: 30818749.
21. Sereti I, Krebs SJ, Phanuphak N, Fletcher JL, Slike B, Pinyakorn S, et al. *Persistent, albeit reduced, chronic inflammation in persons starting antiretroviral therapy in acute HIV infection. Clin Infect Dis* 2017;**64**(2):124–31. https://doi.org/10.1093/cid/ciw683. PubMed PMID: 27737952.
22. De Clercq J, De Scheerder MA, Mortier V, Verhofstede C, Vandecasteele SJ, Allard SD, et al. *Longitudinal patterns of inflammatory mediators after acute HIV infection correlate to intact and total reservoir. Front Immunol* 2024;**14**:1337316. https://doi.org/10.3389/fimmu.2023.1337316. PubMed PMID: 38250083.
23. Lama JR, Ignacio RAB, Alfaro R, Rios J, Cartagena JG, Valdez R, et al. *Clinical and immunologic outcomes after immediate or deferred antiretroviral therapy initiation during primary human immunodeficiency virus infection: the Sabes randomized clinical study. Clin Infect Dis* 2021;**72**(6):1042–50. https://doi.org/10.1093/cid/ciaa167. PubMed PMID: 32107526.
24. de Paula HHS, Ferreira ACG, Caetano DG, Delatorre E, Teixeira SLM, Coelho LE, et al. *Reduction of inflammation and T cell activation after 6 months of cART initiation during acute, but not in early chronic HIV-1 infection. Retrovirology* 2018;**15**(1):76. https://doi.org/10.1186/s12977-018-0458-6. PubMed PMID: 30541557.
25. Kosmider E, Wallner J, Gervassi A, Bender Ignacio RA, Pinto-Santini D, Gornalusse G, et al. *Observational study of effects of HIV acquisition and antiretroviral treatment on biomarkers of systemic immune activation. PLoS One* 2024;**19**(7):e0288895. https://doi.org/10.1371/journal.pone.0288895. PubMed PMID: 38976697.

26. Teer E, Mukonowenzou NC, Essop MF. *HIV, inflammation, and immunometabolism: a model of the inflammatory theory of disease. Viruses* 2025;**17**(6):839. https://doi.org/10.3390/v17060839. PubMed PMID: 40573430.
27. Teer E, Mukonowenzou NC, Essop MF. *The role of immunometabolism in HIV-1 pathogenicity: links to immune cell responses. Viruses* 2022;**14**(8):1813. https://doi.org/10.3390/v14081813
28. Valle-Casuso JC, Angin M, Volant S, Passaes C, Monceaux V, Mikhailova A, et al. *Cellular metabolism is a major determinant of HIV-1 reservoir seeding in CD4 + T cells and offers an opportunity to tackle infection. Cell Metab* 2019;**29**(3):611–26. https://doi.org/10.1016/j.cmet.2018.11.015. PubMed PMID: 30581119.
29. Palmer CS, Cherry CL, Sada-Ovalle I, Singh A, Crowe SM. *Glucose metabolism in T cells and monocytes: new perspectives in HIV pathogenesis. eBioMedicine* 2016;**6**:31–41. https://doi.org/10.1016/j.ebiom.2016.02.012. PubMed PMID: 27211546.
30. Naidoo KK, Highton AJ, Baiyegunhi OO, Bhengu SP, Dong KL, Bunders MJ, et al. *Early initiation of antiretroviral therapy preserves the metabolic function of CD4+ T cells in subtype C human immunodeficiency virus 1 infection. J Infect Dis* 2024;**229**(3):753–62. https://doi.org/10.1093/infdis/jiad432. PubMed PMID: 37804102.
31. Suanzes P, Navarro J, Rando-Segura A, Álvarez-López P, García J, Descalzo V, et al. *Impact of very early antiretroviral therapy during acute HIV infection on long-term immunovirological outcomes. Int J Infect Dis* 2023;**136**:100–6. https://doi.org/10.1016/j.ijid.2023.09.009. PubMed PMID: 37726066.
32. Fiebig EW, Wright DJ, Rawal BD, Garrett PE, Schumacher RT, Peddada L, et al. *Dynamics of HIV viremia and antibody seroconversion in plasma donors: implications for diagnosis and staging of primary HIV infection. AIDS* 2003;**17**:1871–9. https://doi.org/10.1097/01.aids.0000076308.76477.b8
33. Bruner KM, Wang Z, Simonetti FR, Bender AM, Kwon KJ, Sengupta S, et al. *A quantitative approach for measuring the reservoir of latent HIV-1 proviruses. Nature* 2019;**566**(7742):120–5. https://doi.org/10.1038/s41586-019-0898-8. PubMed PMID: 30700913.
34. Kinloch NN, Ren Y, Conce Alberto WD, Dong W, Khadka P, Huang SH, et al. *HIV-1 diversity considerations in the application of the intact proviral DNA assay (IPDA). Nat Commun* 2021;**12**(1):165. https://doi.org/10.1038/s41467-020-20442-3. PubMed PMID: 33420062.
35. Wu G. *Amino acids: metabolism, functions, and nutrition. Amino Acids* 2009;**37**(1):1–17. https://doi.org/10.1007/s00726
36. Forman HJ, Zhang H, Rinna A. *Glutathione: overview of its protective roles, measurement, and biosynthesis. Mol Asp Med* 2009;**30**(1–2):1–12. https://doi.org/10.1016/j.mam.2008.08.006. PubMed PMID: 18796312.
37. Gamarra Y, Santiago FC, Molina-López J, Castaño J, Herrera-Quintana L, Domínguez Á, et al. *Pyroglutamic acidosis by glutathione regeneration blockage in critical patients with septic shock. Crit Care* 2019;**23**(1):162. https://doi.org/10.1186/s13054-019-2450-5. PubMed PMID: 31064391.
38. Patel D, Witt SN. *Ethanolamine and phosphatidylethanolamine: partners in health and disease. Oxid Med Cell Longev* 2017;**2017**:4829180. https://doi.org/10.1155/2017/4829180. PubMed PMID: 28785375.
39. Chaudhry R, Varacallo M. *Biochemistry, glycolysis.* StatPearls [Internet]. Updated 2023 Aug 8. Treasure Island (FL): StatPearls Publishing; 2023. [cited 2026 Mar 28]. ⟨https://www.ncbi.nlm.nih.gov/books/NBK482303/⟩.
40. Roosterman D, Cottrell GS. *Rethinking the citric acid cycle: connecting pyruvate carboxylase and citrate synthase to the flow of energy and material. Int J Mol Sci* 2021;**22**(2):604–17. https://doi.org/10.3390/ijms22020604. PubMed PMID: 33435350.
41. Sano H, Nakamura A, Yamane M, Niwa H, Nishimura T, Araki K, et al. *The polyol pathway is an evolutionarily conserved system for sensing glucose uptake. PLoS Biol* 2022;**20**(6):e3001678. https://doi.org/10.1371/journal.pbio.3001678. PubMed PMID: 35687590.
42. Jain V, Hartogensis W, Bacchetti P, Hunt PW, Hatano H, Sinclair E, et al. *Antiretroviral therapy initiated within 6 months of HIV infection is associated with lower T-cell activation and smaller HIV reservoir size. J Infect Dis* 2013;**208**(8):1202–11. https://doi.org/10.1093/infdis/jit311. PubMed PMID: 23852127.
43. Qin Y, Song T, Su B, Jiao Y, Liu L, Liu Z, et al. *Comparison of HIV DNA decay and immune recovery between early and chronic HIV-infected individuals 96 weeks after ART. HIV Med* 2022;**23**(S1):6–13. https://doi.org/10.1111/hiv.13244
44. Gandhi RT, Cyktor JC, Bosch RJ, Mar H, Laird GM, Martin A, et al. *Intact and defective HIV provirus changes during antiretroviral therapy in people treated during acute or chronic HIV infection or as HIV controllers. Open Forum Infect Dis* 2025;**12**(10):ofaf568. https://doi.org/10.1093/ofid/ofaf568
45. Bruner KM, Murray AJ, Pollack RA, Soliman MG, Laskey SB, Capoferri AA, et al. *Defective proviruses rapidly accumulate during acute HIV-1 infection. Nat Med* 2016;**22**(9):1043–9. https://doi.org/10.1038/nm.4156. PubMed PMID: 27500724.
46. Lee GQ, Reddy K, Einkauf KB, Gounder K, Chevalier JM, Dong KL, et al. *HIV-1 DNA sequence diversity and evolution during acute subtype C infection. Nat Commun* 2019;**10**(1):2737. https://doi.org/10.1038/s41467-019-10659-2. PubMed PMID: 31227699.
47. Cohen MS, Shaw GM, Mcmichael AJ, Ch B, Haynes BF. *Acute HIV-1 Infection. N Engl J Med* 2011;**364**(20):1943–54. https://doi.org/10.1056/NEJMra1011874
48. Harper J, Ribeiro SP, Chan CN, Aid M, Deleage C, Micci L, et al. *Interleukin-10 contributes to reservoir establishment and persistence in SIV-infected macaques treated with antiretroviral therapy. J Clin Investig* 2022;**132**(8):e155251. https://doi.org/10.1172/JCI155251. PubMed PMID: 35230978.
49. Wilson EB, Brooks DG. *The role of IL-10 in regulating immunity to persistent viral infections. Curr Top Microbiol Immunol* 2011;**350**:39–65. https://doi.org/10.1007/82_2010_96
50. Liu J, Zhan W, Kim CJ, Clayton K, Zhao H, Lee E, et al. *IL-10-producing B cells are induced early in HIV-1 infection and suppress HIV-1-specific T cell responses. PLoS One* 2014;**9**(2):e89236. https://doi.org/10.1371/journal.pone.0089236. PubMed PMID: 24586620.
51. Löffek S, Schilling O, Franzke CW. *Series 'matrix metalloproteinases in lung health and disease': biological role of matrix metalloproteinases: a critical balance. Eur Respir J* 2011;**38**(1):191–208. https://doi.org/10.1183/09031936.00146510. PubMed PMID: 21177845.
52. Tokunaga R, Zhang W, Naseem M, Puccini A, Berger MD, Soni S, et al. *CXCL9, CXCL10, CXCL11/CXCR3 axis for immune activation – a target for novel cancer therapy. Cancer Treat Rev* 2018;**63**:40–7. https://doi.org/10.1016/j.ctrv.2017.11.007. PubMed PMID: 29207310.
53. Lisco A, Introini A, Munawwar A, Vanpouille C, Grivel JC, Blank P, et al. *HIV-1 imposes rigidity on blood and semen cytokine networks. Am J Reprod Immunol* 2012;**68**(6):515–21. https://doi.org/10.1111/aji.12015. PubMed PMID: 23006048.
54. De La Torre Tarazona E, Moraga E, Fons-Contreras M, Vaquer R, Sánchez-Palomino S, Vallejo-Palma G, et al. *Identification of inflammation markers as novel potential predictors of the HIV-DNA reservoir size. Int J Mol Sci* 2025;**26**(17):8430. https://doi.org/10.3390/ijms26178430. PubMed PMID: 40943350.
55. Kang S, Tang H. *HIV-1 infection and glucose metabolism reprogramming of T cells: another approach toward functional cure and reservoir eradication. Front Immunol* 2020;**11**:572677. https://doi.org/10.3389/fimmu.2020.572677. PubMed PMID: 33117366.
56. Shoulders MD, Raines RT. *Collagen structure and stability. Annu Rev Biochem* 2009;**78**:929–58. https://doi.org/10.1146/annurev.biochem.77.032207.120833. PubMed PMID: 19344236.
57. Spangenberg SH, Palermo A, Gazaniga NR, Martínez-Peña F, Guijas C, Chin EN, et al. *Hydroxyproline metabolism enhances IFN-γ-induced PD-L1 expression and inhibits autophagic flux. Cell Chem Biol* 2023;**30**(9):1115–34. https://doi.org/10.1016/j.chembiol.2023.06.016. PubMed PMID: 37467751.
58. Porichis F, Kwon DS, Zupkosky J, Tighe DP, Mcmullen A, Brockman MA, et al. *Responsiveness of HIV-specific CD4 T cells to PD-1 blockade. Blood* 2011;**118**(4):965–74. https://doi.org/10.1182/blood-2010-12-328070
59. Zhang QS, Wang JN, Yang TL, Li SY, Li JQ, Liu DN, et al. *SHMT2 regulates CD8+ T cell senescence via the reactive oxygen species axis in HIV-1 infected patients on antiretroviral therapy. eBioMedicine* 2025;**112**:105533. https://doi.org/10.1016/j.ebiom.2024.105533. PubMed PMID: 39808948.
60. Yahsi B, Gunaydin G. *Immunometabolism – the role of branched-chain amino acids. Front Immunol* 2022;**13**:886822. https://doi.org/10.3389/fimmu.2022.886822. PubMed PMID: 35812393.
61. Besnard E, Hakre S, Kampmann M, Lim HW, Hosmane NN, Martin A, et al. *The mTOR complex controls HIV latency. Cell Host Microbe* 2016;**20**(6):785–97. https://doi.org/10.1016/j.chom.2016.11.001. PubMed PMID: 27978436.
62. Huarte N, Carravilla P, Cruz A, Lorizate M, Nieto-Garai JA, Kräusslich HG, et al. *Functional organization of the HIV lipid envelope. Sci Rep* 2016;**6**:34190. https://doi.org/10.1038/srep34190